



Parametric Study of Hole Pattern Influence on Average Bending Stiffness

Robert S. Glauz, P.E.¹

Abstract

The presence of holes in cold-formed steel structural members reduces the global buckling capacity. Current design provisions in the North American Specification for the design of cold-formed steel members utilize a simple reduction in member stiffness caused by holes. The cross-section moment of inertia is a weighted average of the gross and net section values, but this is restricted to cases where the hole locations are symmetric about the midpoint of the member. For other hole patterns, the Commentary provides a more precise calculation using an exhaustive summation over the member length considering each hole location. In practice, it is common to have uniformly spaced holes, but not necessarily centered across the member. The purpose of this investigation is to assess the impact of offset and other hole patterns, and determine if the simple weighted average method can be extended for broader application.

1. Introduction

Cold-formed steel structural members commonly have holes to provide passageways for utilities in residential and midrise construction. These holes are typically pre-punched in the members with uniform spacing as shown in Figure 1. These holes can reduce the structural capacity of the member for a variety of failure modes, including global buckling.

The AISI Specification (2016) provides a convenient method of calculating the bending stiffness of a member with holes for use in predicting the global buckling capacity. However, this simple calculation is restrictive in its application, requiring the hole pattern to be symmetric about the midpoint of the member. This report presents the results of parametric studies performed to evaluate the characteristics of hole patterns and how they influence the average bending stiffness. A series of recommendations are made to improve the current AISI provisions and broaden their applicability.

¹ President/Owner, RSG Software, Inc., glauz@rsgsoftware.com

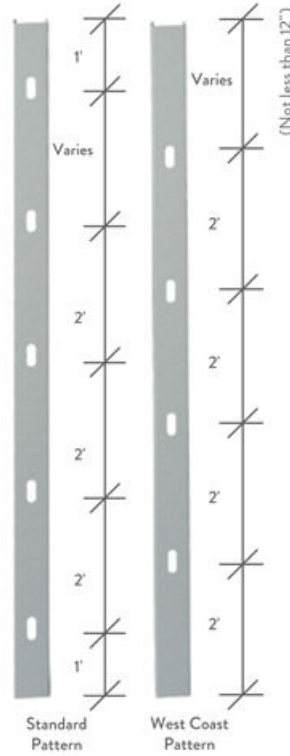


Figure 1. Example stud hole patterns. Source: ClarkDietrich (2017)

2. Background

The AISI Specification (2016) provisions for reduced bending stiffness were based on the extensive work by Moen and Schafer (2009). A Rayleigh-Ritz energy solution was employed for buckling of a general column with n arbitrarily spaced holes as shown in Figure 2, whereby the external work of an applied axial force, P , was equated to the strain energy due to flexure.

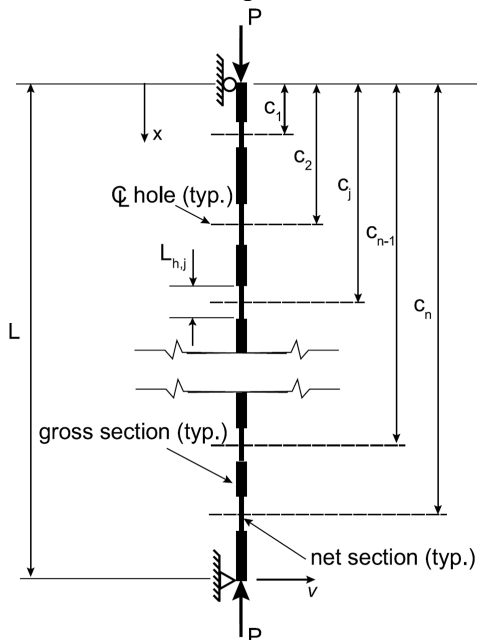


Figure 2. Column definition and notation

This development assumed a half-sinewave displacement function. This is accurate for a prismatic member, but variations in bending stiffness throughout the member alter this buckled shape. However, the localized reductions in stiffness are typically not large, so the assumed displacement function remains a very good approximation which was validated in Moen and Schafer (2009).

The resulting critical elastic buckling load, P_{cre} , is shown as Eq. 1, where I_g and I_{net} are the moments of inertia for the gross and net sections respectively, L_g and L_{net} are the total lengths of the gross and net section regions respectively, and I_{avg} is the average moment of inertia for buckling. This equation includes a trigonometric term, T , shown in Eq. 2. This expression for T reflects a correction to that in Moen and Schafer (2009) which had 2π in the denominator.

$$P_{cre} = \frac{\pi^2 E}{L^2} \left[\frac{I_g L_g + I_{net} L_{net} + T(I_g - I_{net})}{L} \right] = \frac{\pi^2 E}{L^2} I_{avg} \quad (1)$$

$$T = \frac{L}{\pi} \sum_{j=1}^n \cos\left(\frac{2\pi c_j}{L}\right) \sin\left(\frac{\pi L_{h,j}}{L}\right) \quad (2)$$

The expression for T can be represented graphically as shown in Figure 3, where T is the sum of the areas under the curve for the net section regions. Figure 3a shows an arbitrary set of hole locations and sizes where T is generally non-zero.

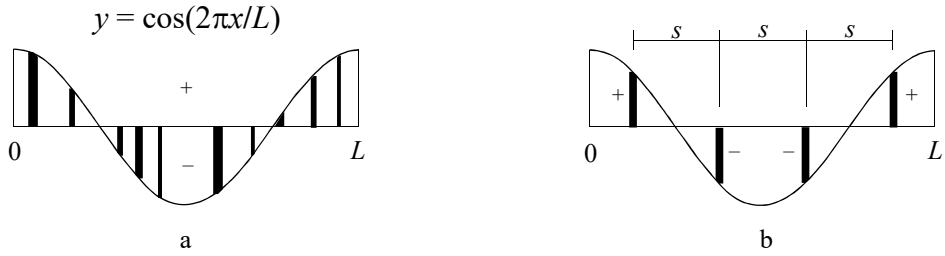


Figure 3. Graphical representation of term T

For a column with n identical holes at uniform spacing, s , where $L = n s$ and the hole pattern is centered as shown in Figure 3b, the term T is equal to zero. This reduces Eq. 1 to Eq. 3 where $I_{wt.avg}$ is the simple “weighted average” moment of inertia independent of hole distribution.

$$P_{cre} = \frac{\pi^2 E}{L^2} \left[\frac{I_g L_g + I_{net} L_{net}}{L} \right] = \frac{\pi^2 E}{L^2} I_{wt.avg} \quad (3)$$

3. Investigation

This study evaluates how different hole distributions influence I_{avg} as compared to $I_{wt.avg}$. The ratio $I_{avg} / I_{wt.avg}$ is a measure of the theoretical error in buckling load if $I_{wt.avg}$ is used instead of I_{avg} . For ratios less than 1, $I_{wt.avg}$ overpredicts the buckling load and is therefore unconservative.

3.1 Single Hole

For a member with only one hole, $L_{net} = L_h$. If L_h is relatively small, $\sin(\pi L_h/L) \approx \pi L_h/L$, therefore:

$$T = L_{net} \cos\left(\frac{2\pi c}{L}\right) \quad (4)$$

Using a representative value of $I_{net} / I_g = 0.7$, the ratio $I_{avg} / I_{wt.avg}$ varies with the location and size of the hole as reflected in Figure 4.

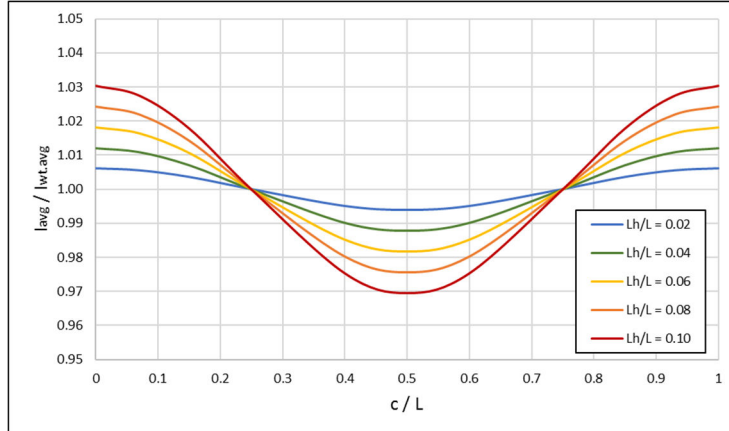


Figure 4.

For cases where the hole is near the ends of the member, $I_{wt.avg}$ is conservatively low. For cases where the hole is near the middle, $I_{wt.avg}$ is unconservatively high. This is the expected result because the buckled shape has more curvature, and thus more bending, near the middle. If the hole is located at the middle of the member, $T = -L_{net}$, resulting in the average moment of inertia shown in Eq. 5. This represents a lower bound for all possible hole locations and distributions.

$$I_{avg} = I_g - 2(I_g - I_{net}) L_{net}/L \quad (5)$$

The expression for $I_{wt.avg}$ can be restated as shown in Eq. 6. If a small amount of error, e , was permitted, equating the ratio $I_{avg} / I_{wt.avg}$ to $(1 - e)$ provides a limit on L_{net} shown in Eq. 7.

$$I_{wt.avg} = I_g - (I_g - I_{net}) L_{net}/L \quad (6)$$

$$L_{net} \leq \left(\frac{e}{1+e}\right) \frac{L}{1-I_{net}/I_g} \quad (7)$$

3.2 Symmetric Patterns

The AISI provision for weighted average moment of inertia requires the hole pattern to be symmetric about the midpoint. This results in a symmetrical buckled shape, but it does not ensure that the average moment of inertia is accurate. Figure 5 illustrates two symmetrical hole patterns where T is not equal to zero.



Figure 5. Symmetrical hole patterns

In Figure 5a, the area of the negative net section regions exceeds the area of the positive net section regions, so T is less than zero. In Figure 5b, the area of the positive net section regions exceeds the area of the negative net section regions, so T is greater than zero. The requirement that the hole pattern be symmetric about the midpoint is therefore not suitable.

3.3 Uniform Spacing of Identical Holes

It is common for cold-formed steel members to have repeating holes at a constant spacing. Figure 6a illustrates the magnitude of T for an example with 5 holes, where $L = 5s$.

The expression for T in Eq. 2 contains $\sin(\pi L_h/L)$ which is constant for all holes. Therefore, the sum requires only the cosine term, and for evenly spaced values the sum of the cosines is equal to zero. This can be demonstrated using the diagram in Figure 6b.

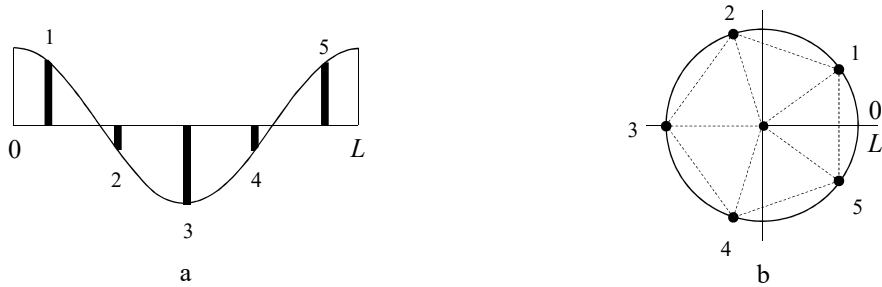


Figure 6. Uniform centered hole pattern

The locations of the holes are plotted as evenly spaced points on a circle. The x coordinates of these points are the cosines of the values, and the y coordinates are the sines of the values. By symmetry it is evident that the average of the points is the center of the circle. Therefore, the sum of the cosines must be zero, resulting in $T=0$.

If this uniform spacing is not centered, as in Figure 7a, the hole pattern is no longer symmetrical. However, the circle plot in Figure 7b demonstrates that the sum of the cosines is still zero. Therefore $T=0$ regardless of the offset magnitude. This deduction can be generalized to n identical holes at uniform spacing s , where $L = n s$.

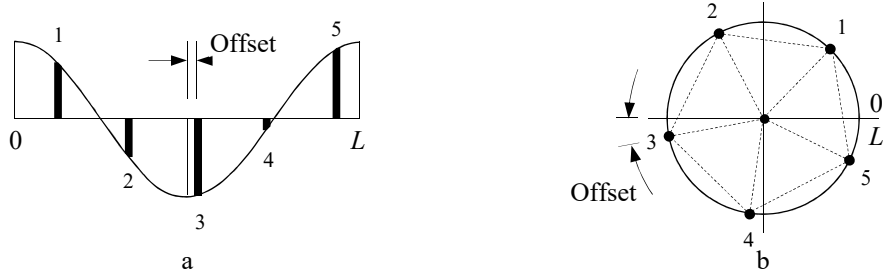


Figure 7. Uniform offset hole pattern

3.4 Length Variations

If the hole spacing is uniform but the length is not a multiple of the spacing, T is not equal to zero. For lengths less than ns as shown in Figure 8a, the holes are farther from the middle so T is positive. For lengths greater than ns as shown in Figure 8b, the holes are closer to the middle so T is negative. As a result, $I_{avg} < I_{wt.avg}$ so using $I_{wt.avg}$ would be unconservative. Figure 9 illustrates how this ratio varies for the case of $n = 5$ using a representative value of $L_h/s = 0.3$.



Figure 8. Length not a multiple of spacing

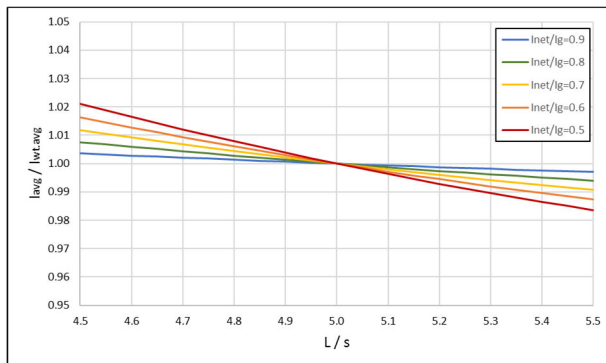


Figure 9. Impact of length variation for $n = 5$ and $L_h/s = 0.3$

3.5 Hole Size and Spacing

The previous sections explored the impact of hole patterns, offsets, and member length variations. To gain a more complete understanding for uniform spacing, these observations are combined with variations in hole size, spacing, and the ratio I_{net} / I_g , as illustrated in the charts of Figure 10.

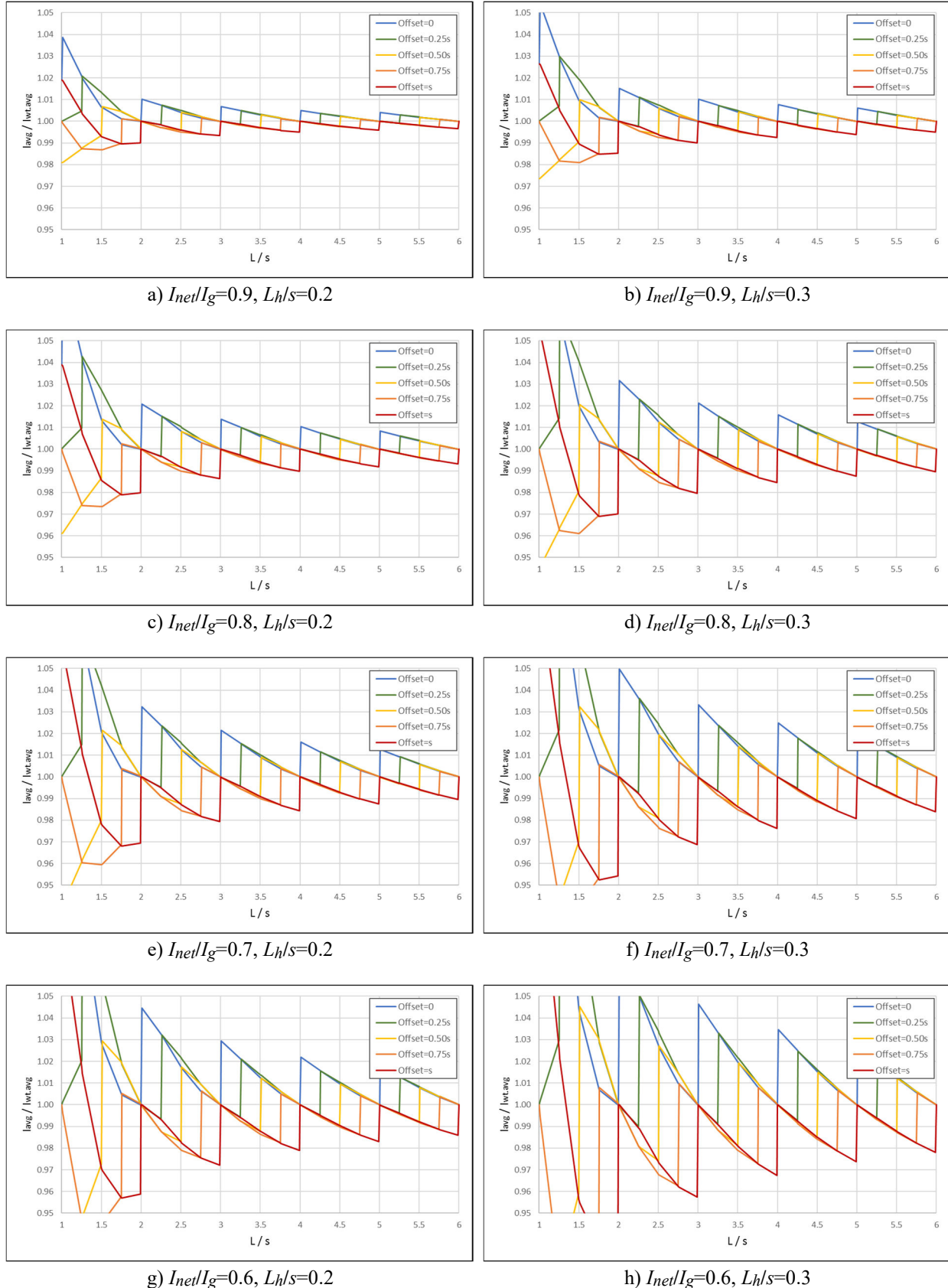


Figure 10. Impact of various hole patterns

The *Offset* in these charts is defined as the distance from the end of the member to the first hole, and therefore $n = (L - \text{Offset}) / s$ rounded up. As expected, smaller errors occur with higher values of I_{net}/I_g , lower values of L_h/s , and greater n . The controlling curve is for $\text{Offset} = s$, where the first hole is farther from the end of the member.

Many of the cases where L/s is less than 2 are unconservative because they have only one hole. For these cases Section 3.1 for single holes should be referenced. For L/s greater than 2, the worst case is for two holes located at $\frac{1}{3}L$ and $\frac{2}{3}L$. For this case:

$$T = \frac{L}{\pi} 2 \cos\left(\frac{2\pi}{3}\right) \frac{\pi L_h}{L} = -L_h = -L_{net}/2 \quad (8)$$

$$I_{avg} = I_g - 1.5(I_g - I_{net}) L_{net}/L \quad (9)$$

This can be generalized further for n holes as shown in Eq. 10. Then for a permitted amount of error, e , the limit on L_h can be expressed as shown in Eq. 11. This is equivalent to Eq. 7 for the case of $n = 1$. Finally, an approximation of Eq. 11 for small values of e provides a simpler form as Eq. 12.

$$I_{avg} = I_g - (1 + \frac{1}{n})(I_g - I_{net}) L_{net}/L \quad (10)$$

$$L_h \leq \left(\frac{e}{1+ne}\right) \frac{L}{1-I_{net}/I_g} \quad (11)$$

$$L_h \leq \frac{eL}{1-I_{net}/I_g} \quad (12)$$

3.6 Varying Hole Sizes and Spacing

The previous section applies to uniform spacing of identical holes. Although the general form in Eq. 1 is applicable to nonuniform spacings and hole sizes, it requires a single value for I_{net} . A more general form which permits different values of I_{net} can be expressed as follows:

$$I_{avg} = I_g - \sum_{j=1}^n (I_g - I_{net,j}) \left(\frac{L_{h,j}}{L} - \frac{1}{\pi} \cos \frac{2\pi c_j}{L} \sin \frac{\pi L_{h,j}}{L} \right) \quad (13)$$

For relatively small values of L_h , $\sin(\pi L_h/L) \approx \pi L_h/L$. This can be used to simplify Eq. 13 to the following:

$$I_{avg} = I_g - \sum_{j=1}^n (I_g - I_{net,j}) \left(1 - \cos \frac{2\pi c_j}{L} \right) \frac{L_{h,j}}{L} \quad (14)$$

Figure 11 illustrates the influence of the term $(1 - \cos 2\pi c_j/L)$. Holes near the middle of the member have the most reduction to the average stiffness, whereas holes near the ends have little impact.

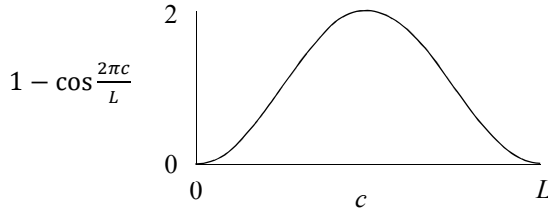


Figure 11. Influence of hole location

3.7 Other Boundary Conditions

The development of the average moment of inertia by Moen and Schafer (2009) was based on a simply-supported column with pinned end conditions, where the displacement function was a half-sinewave. The more general form of the displacement function for other boundary conditions is:

$$u = a_1 \sin \frac{\pi x}{L_e} + a_2 \cos \frac{\pi x}{L_e} + a_3 x + a_4 \quad (15)$$

where L_e is the half-wavelength, or the effective length, of the column. The strain energy due to flexure is determined using the second derivative of the displacement:

$$u'' = -a_1 \frac{\pi^2}{L_e^2} \sin \frac{\pi x}{L_e} - a_2 \frac{\pi^2}{L_e^2} \cos \frac{\pi x}{L_e} \quad (16)$$

Through trigonometric relationships, this can be restated as a shifted sine curve:

$$u'' = -A \frac{\pi^2}{L_e^2} \sin \frac{\pi(x+x_o)}{L_e} \quad (17)$$

$$\text{where } A = \sqrt{a_1^2 + a_2^2} \quad x_o = \frac{L_e}{\pi} \arctan \frac{a_2}{a_1} \quad (18)$$

Therefore, this is identical to the analysis in Section 3.5 if an additional offset is used for each hole location. Consequently, the limit on L_h defined in Eqs. 11 and 12 are still applicable for other boundary conditions if holes are uniformly spaced.

3.8 Torsional Buckling

All the preceding investigations address the impact of holes on the bending stiffness used for flexural buckling. Many cold-formed steel members are also subject to torsional buckling, which is a function of two other properties of the cross-section: St. Venant torsion constant, J , and warping torsion constant C_w . The torsion strain energy where pure torsion and warping torsion both exist is given by:

$$U = \frac{1}{2} \int_0^L GJ(\phi')^2 dx + \frac{1}{2} \int_0^L EC_w(\phi'')^2 dx \quad (19)$$

For the simply-supported case, the displacement function for angle of twist, ϕ , is a sine curve, just as for flexure. The first derivative is a cosine curve, and the integration for pure torsion results in a trigonometric term equal to $-T$. This is the reverse of the impact on the weighted average for flexural buckling. Holes near the ends of the member reduce J_{avg} more than holes near the middle, and the plots of Figure 10 would be inverted for $J_{avg}/J_{wt.avg}$.

For uniformly spaced holes, the amount of error, e , can still be enforced using the approximate limit on L_h defined in Eq. 12. The general form for J_{avg} is similar to Eq. 14, but with the cosine term negated:

$$J_{avg} = J_g - \sum_{j=1}^n (J_g - J_{net,j}) \left(1 + \cos \frac{2\pi c_j}{L} \right) \frac{L_{h,j}}{L} \quad (20)$$

For the torsional warping term, the strain energy uses the second derivative of the displacement function, which is identical to flexure. Therefore, the impact of holes on the weighted average of C_w follows the same behavior observed for the average moment of inertia, I_{avg} . However, the work by Moen and Schafer (2009) determined that the weighted average warping constant overestimates the warping stiffness due to the disruption of warping stresses at hole locations. As a result, the current AISI (2016) provisions conservatively use the net section C_w .

4. Recommendations

The current AISI provisions for using $I_{avg} = I_{wt.avg}$ are restricted to cases where the hole pattern is symmetric about the midpoint of the member. Based on the findings above, these provisions should be changed to permit the weighted average moment of inertia for any member with uniformly spaced holes, within some limits. This is correct for cases where $L = n s$, but slightly off for other cases. To accommodate different lengths and hole pattern offsets, it is reasonable to permit a small amount of unconservative error. It is recommended that a 2% error be allowed, which can be enforced using the following relationship obtained from Eq. 12:

$$L_h \leq \frac{0.02L}{1 - I_{net}/I_g} \quad (21)$$

SSMA (2015) defines a variety of standard sections with common size web holes. The ratio I_{net}/I_g varies from 0.975 to 0.999 for bending about the major axis, and varies from 0.802 to 0.985 for bending about the minor axis. For an extreme case using $I_{net}/I_g = 0.8$ and $L = 48$ inches, the above equation limits L_h to 4.8 inches, which is greater than the current AISI limit of 4.5 inches.

For non-uniformly spaced holes, it is recommended that the provisions permit a conservative value of I_{avg} as calculated using Eq. 5, but not less than I_{net} . The engineer still has the option to use the more accurate method provided in Appendix 2 of the Commentary, although a correction to the expression for T is required. To properly handle members with varying net sections, the more general form of Eq. 14 should be provided.

The general equation for the average torsion constant is slightly different from the equation for moment of inertia. But for uniformly spaced holes, the relationship between L_h and the potential error remains the same. Therefore, it is recommended that Eq. 21 be applied as a limit for $J_{avg}=J_{wt.avg}$. The general form of Eq. 20 should also be provided in the Commentary.

5. Conclusions

The use of a simple weighted average moment of inertia can be used in broader applications to approximate the bending stiffness used for global buckling calculations. The current AISI provisions limit this approach to hole patterns symmetrical about the midpoint. This study demonstrated that symmetry is not a suitable criterion. Rather uniform spacing is the important factor, which happens to align better with common practice.

This investigation provides recommendations for changes to the AISI Specification which simplify the calculations required by the engineer. A minor correction is required to the AISI Commentary for the general case, and a more general form is provided which should benefit the engineer for cases with different net sections.

References

- American Iron and Steel Institute (2016), *North American Specification for the Design of Cold-Formed Steel Structural Members*, 2016 Edition, Washington, DC, 2016.
- Moen, C.D. and Schafer, B.W. (2009), "Elastic Buckling of Cold-Formed Steel Columns and Beams with Holes," *Engineering Structures*, 31(12), pp.2812-2824, 2009.
- Glauz, R.S. (2017), "Flexural-Torsional Buckling of General Cold-Formed Steel Columns with Unequal Unbraced Lengths," *Thin-Walled Structures*, 2017.
- Timoshenko, S.P. and Gere, J.M. (1961), *Theory of Elastic Stability*, 2nd Edition, McGraw-Hill, New York, NY, 1961.
- Yoo, C.H. and Lee, S.C. (2011), *Stability of Structures: Principles and Applications*, 1st Edition, Butterworth-Heinemann, Elsevier Inc., 2011.
- Steel Stud Manufacturers Association (2015), *Product Technical Guide*, SSMA, Chicago, IL, 2015.
- ClarkDietrich (2017), *Structural Studs*, <http://www.clarkdietrich.com/products/curtain-wall-framing/structural-studs>, Clarkwestern Dietrich Building Systems LLC, 2017.
- CRC Press (1976), *Standard Mathematical Tables*, 24th Edition, CRC Press, Inc., West Palm Beach, FL, 1976.

Appendix 1 –Derivation for Uniform Spacing

The general form for the average moment of inertia with uniform spacing of identical holes is:

$$I_{avg} = I_g - (I_g - I_{net}) \frac{L_h}{L} \sum_{j=0}^{n-1} \left(1 - \cos \frac{2\pi(c_1 + js)}{L} \right)$$

The sum of cosines can be condensed into one expression using the derivation by Knapp (2009):

$$\sum_{j=0}^{n-1} \cos \frac{2\pi(c_1 + js)}{L} = \frac{\sin \frac{\pi ns}{L}}{\sin \frac{\pi s}{L}} \cos \left(\frac{\pi(2c_1 + (n-1)s)}{L} \right)$$

The sine terms can be approximated for small angles as follows:

$$\begin{aligned} \sin \frac{\pi ns}{L} &= \sin \left(\pi - \frac{\pi ns}{L} \right) \cong \frac{\pi(L - ns)}{L} \\ \sin \frac{\pi s}{L} &\cong \frac{\pi s}{L} \end{aligned}$$

The cosine term can make use of $2c_1 + (n-1)s \cong L$:

$$\begin{aligned} \cos \left(\frac{\pi(2c_1 + (n-1)s)}{L} \right) &\cong \cos \pi = -1 \\ \sum_{j=0}^{n-1} \left(1 - \cos \frac{2\pi(c_1 + js)}{L} \right) &\cong n - \frac{L - ns}{s}(-1) = \frac{L}{s} \end{aligned}$$

This leads to the following simple form, which is much more accurate than the weighted average. For practical cases, overestimation of I_{avg} is less than 0.03%. For an extreme case using $n = 2$, $L_h/s = 0.5$ and $I_{net}/I_g = 0.8$, the largest overestimation of I_{avg} is less than 0.5%.

$$I_{avg} = I_g - (I_g - I_{net}) \frac{L_h}{s}$$

Reference

Knapp, M.P. (2009), “Sines and Cosines of Angles in Arithmetic Progression,” *Mathematics Magazine*, Vol. 82, pp.371-372, 2009.